Paramagnetic-Resonance Absorption of Ions with Spin 5/2: Mn^{++} in Calcite

CHIHIRO KIKUCHI*

Department of Nuclear Engineering, University of Michigan, Ann Arbor, Michigan

AND

L. M. MATARRESE†

Solid State Division, Naval Research Laboratory, Washington 25, D. C.

(Received February 25, 1960)

The theory of the paramagnetic-resonance absorption of ions with $S=\frac{5}{2}$ in crystalline fields of trigonal symmetry is presented. The case of manganous ions in calcite ($CaCO_3$) is taken as an example. It is shown that the splitting of the fine-structure satellites into doublets first reported by Hurd, Sachs, and Hershberger [Phys. Rev. **93**, 373 (1954)] can be accounted for by assuming that the manganous ions can occupy the two nonequivalent Ca^{++} sites at random. The maximum splitting was measured at X band and K band and found to be 19.3±0.5 gauss. The value computed from the theory, assuming an ionic model, is 23.8 gauss. In addition, five pairs of weak lines were found, each pair occurring midway between adjacent hyperfine groups. The origin of these lines is uncertain. The applicability of the present theory to Al_2O_3:Fe, a zero-field maser material, and to the photosensitive Fe^{+++} center in CdS is pointed out.

INTRODUCTION

IN a paper on the paramagnetic-resonance absorption spectrum of Mn^{++} in single crystals of $CaCO_3$ of the calcite structure, Hurd, Sachs, and Hershberger[1] reported the splitting of the Mn^{++} fine-structure lines into doublets. According to their observations, the doublet separations depend upon the orientation of the applied magnetic field with respect to the crystal, the splitting being most pronounced at about 60° with respect to the trigonal c axis, and decreasing to zero at 0° and 90°. Furthermore, it was noted that the strong fine-structure lines are split into wider doublets than the weak ones.

The explanation of this effect was provided independently by one of the present authors[2] and by McConnell.[3] The doublet structure results from the difference in the crystalline electric fields at the two nonequivalent Ca^{++} sites occupied by the Mn^{++} ions. Because of the three-fold symmetry about the c axis, the crystalline electric field potential contains the non-axial harmonics $Y_{4\pm3}$ in addition to the axial harmonics considered by HSH. It will be the purpose of this paper to show that by including terms which transform like $Y_{4\pm3}$, it is possible to account for their results. Additional results have been reported by Kikuchi, Ager, and Matarrese.[4]

Although in the above references the problem of Mn^{++} ions in calcite was dealt with, the same general arguments are applicable to all paramagnetic ions of spin $\frac{5}{2}$ in a trigonal field. One example is Fe^{+++} in corundum ($\alpha-Al_2O_3$), a material which recently has attracted considerable attention because of its usefulness as a material for a zero-field maser.[5] Because the spin of Fe^{+++} is $\frac{5}{2}$, the Fe^{+++} ions occupying the nonequivalent Al^{+++} sites in corundum become distinguishable, in contrast to the Cr^{+++} ions, which are all magnetically equivalent because the spin is only $\frac{3}{2}$. Another example is the photosensitive iron center in CdS reported by Lambe, Baker, and Kikuchi.[6] In this case, the effects due to the crystalline electric field are large and the line width is narrow, so that the second-order splitting of the $-\frac{1}{2}\leftrightarrow\frac{1}{2}$ line is observed.

Thus, because of the growing interest in the problem of paramagnetic ions of spin $\frac{5}{2}$ in a field of trigonal symmetry, the present paper was undertaken to present some of the theoretical and experimental details which have hitherto not been published.

CALCIUM SITES

The rhombohedral unit cell of calcite is shown in Fig. 1. The crystal constants are $a_0=6.361$ A and $\alpha=46°6'$, and c_0'', the length of the unit cell along the trigonal c axis, is 17.020 A. The carbonates and calcium ions contained in a unit cell are designated by A, B, and P, Q, respectively. These ions lie in separate layers normal to the c axis, such that the stacking sequence is $BPAQ$, with spacing $c_0''/12$. The hexagonal prisms in Fig. 1 show the different arrangements of the carbonates about the P and Q calcium sites. In order to make clear the difference between the calcium sites, the top and bottom of each prism are shown in greater detail in Fig. 2. According to x-ray analysis, carbonate oxygens form an equilateral triangle with 1.26 A as the carbon-oxygen distance. Further, the carbonates

* Supported in part by Air Force Office of Scientific Research and Project Michigan.

† Part of the contribution of this author is based on work done at Lawrence Radiation Laboratory, Livermore, California, summer, 1959.

[1] F. K. Hurd, M. Sachs, and W. D. Hershberger, Phys. Rev. **93**, 373 (1954); referred to hereafter as HSH.

[2] C. Kikuchi, Phys. Rev. **100**, 1243 (1955).

[3] H. M. McConnell, J. Chem. Phys. **24**, 904 (1956).

[4] C. Kikuchi, R. Ager, and L. M. Matarrese, Bull. Am. Phys. Soc. Ser. II, **3**, 135 (1958).

[5] J. King and R. W. Terhune, J. Appl. Phys. **30**, 1844 (1959).

[6] J. Lambe, J. Baker, and C. Kikuchi, Phys. Rev. Letters **3**, 270 (1959).

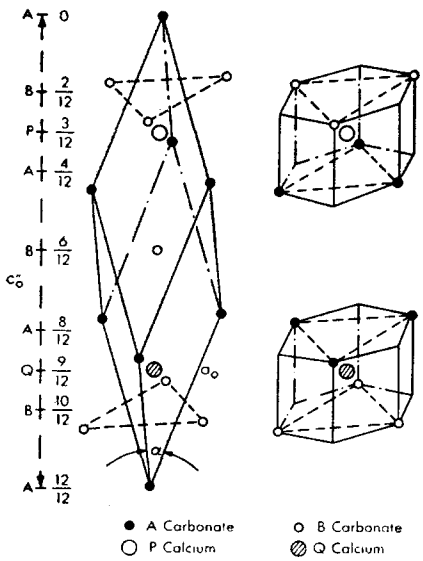

FIG. 1. Unit cell of calcite.

of type B are related to those of type A by an inversion with respect to the central carbon.

One can think of the nearest oxygens as being situated on the alternate vertices of a hexagonal prism. Then Fig. 2 shows that these prisms are different for the sites P and Q; if λ_1 is the angular displacement of the nearest oxygen with respect to the carbons, as shown in the figure, then the relative angular displacement of the two prisms is $2\lambda_1$. The crystalline electric fields at the sites P and Q can be thought of as consisting of contributions from the carbons and the first, second-, and third-nearest oxygens, each set of ions being situated on the alternate vertices of a hexagonal prism. Figure 3 shows two of these prisms. It can be seen that a reflection in the vertical reflection plane

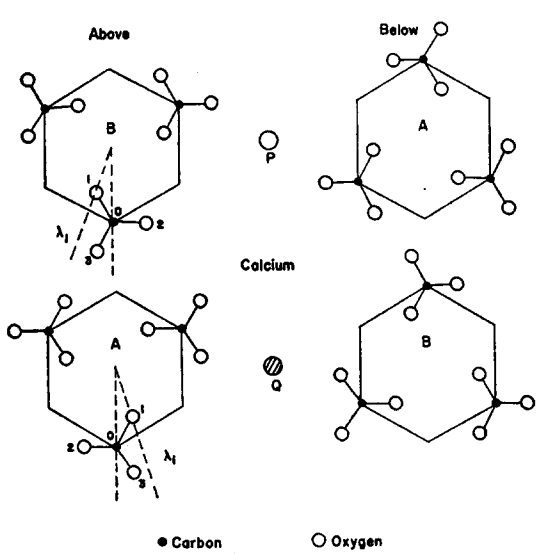

FIG. 2. Carbonates about Ca^{++} sites.

whose trace is shown in the figure changes a P site into a Q site.

CRYSTALLINE ELECTRIC FIELD

The ions located at lattice sites produce an electrostatic field at the position of the electrons localized about the paramagnetic ions. The general form of the crystalline field potential that meets the requirements of crystal symmetry, namely that the field be (1) real, (2) invariant under rotation $\pm 2\pi/3$ about the c axis,

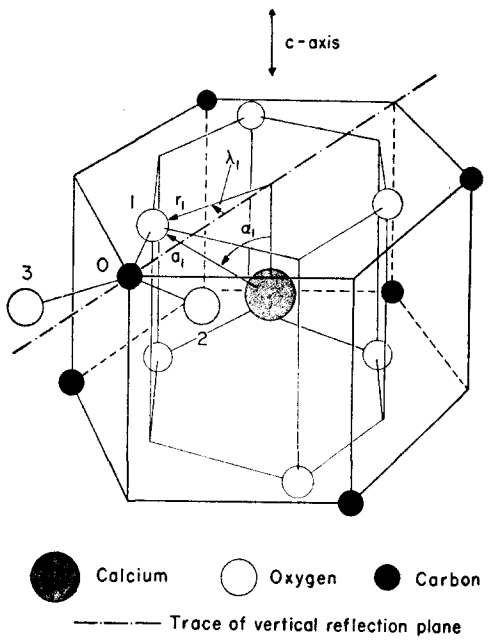

FIG. 3. Calcite hexagonal cell; a P site is shown.

and (3) invariant under rotation $\pi/3$ followed by reflection in a plane normal to the c axis, is given by

$$V=a_{20}Y_{20}+a_{40}Y_{40}+a_{43}Y_{43}+a_{4-3}Y_{4-3}+a_{60}Y_{60}+a_{63}Y_{63}+a_{6-3}Y_{6-3}+a_{66}Y_{66}+a_{6-6}Y_{6-6}+\cdots, \quad (1)$$

in which the Y_{lm} are spherical harmonics and

$$a_{l-m}=(-1)^m a_{lm}^*. \quad (2)$$

For rare-earth ions all of the above terms need to be taken into account; for the iron-group ions, the contribution from spherical harmonics of degree six and higher vanishes, so that the general form of the crystalline electric field can be written

$$V=a_{20}Y_{20}+a_{40}[Y_{40}+b_3Y_{43}-b_3^*Y_{4-3}]. \quad (3)$$

For calcite, if one considers the electrostatic field at the central ion due to the six nearest carbonates, it can be shown that

$$b_{\pm 3}=\frac{\sum_s (Z_s/a_s^5)\bar{P}_{4\pm 3}(\cos\alpha_s)\,\exp(\mp 3i\lambda_s)}{\sum_s (Z_s/a_s^5)\bar{P}_{40}(\cos\alpha_s)}, \quad (4)$$

in which the $\bar{P}_{lm}$ are the normalized associated Legendre

polynomials. The index s refers to the different hexagonal prisms delineated by the carbons and oxygens; Z_s is the charge assigned to the corner ion, and the quantities a_s, α_s, and λ_s are the coordinates of the ion, as exemplified in Fig. 3, for the prism of the first-nearest oxygens. As will be seen later, the parameter that enters directly into the expression for the doublet splitting is

$$b\equiv -(2i)^{-1}(b_3-b_3^*), \tag{5}$$

so that

$$b=\frac{\sum_s(Z_s/a_s^5)\bar{P}_{43}(\cos\alpha_s)\ \sin 3\lambda_s}{\sum_s(Z_s/a_s^5)\bar{P}_{40}(\cos\alpha_s)}. \tag{6}$$

This equation gives us the opportunity to compare the value of b computed from crystallographic data with that obtained from the observed doublet splittings.

MATRIX ELEMENTS

Although the above expressions for the crystalline electric field are written in terms of Y_{lm}, these spherical harmonics are used merely to indicate the transformation properties of the crystalline electric field operator. To obtain the explicit expression for the spin operator, a scheme such as that suggested by Bleaney and Stevens[7] can be used. An alternative procedure is suggested by the property that the Y_{lm} transform like the operators $T_q^{(l)}$ generated by the process[8]

$$T_{q-1}^{(l)}=[l(l+1)-q(q-1)]^{-\frac{1}{2}}[S_-, T_q^{(l)}]. \tag{7}$$

If we set

$$T_2^{(2)}=6^{-\frac{1}{2}}S_+^2, \tag{8}$$

then

$$T_{\pm 1}^{(2)}=\mp 6^{-\frac{1}{2}}(S_zS_\pm+S_\pm S_z),$$

$$T_0^{(2)}=[S_z^2-\tfrac{1}{3}S(S+1)],$$

and

$$T_{-2}^{(2)}=6^{-\frac{1}{2}}S_-^2. \tag{9}$$

Taking

$$T_4^{(4)}=\tfrac{1}{1\,6}(70)^{\frac{1}{2}}S_+^4, \tag{10}$$

we get

$$T_{\pm 3}^{(4)}=\mp\tfrac{1}{8}(35)^{\frac{1}{2}}S_\pm^3(2S_z\pm 3),$$

$$T_{\pm 2}^{(4)}=-\tfrac{1}{8}(10)^{\frac{1}{2}}S_\pm^2[S(S+1)-7S_z^2\mp 14S_z-9],$$

$$T_{\pm 1}^{(4)}=\mp\tfrac{1}{8}(5)^{\frac{1}{2}}S_\pm(2S_z\pm 1)\times[-3S(S+1)+6+7S_z^2\pm 7S_z],$$

$$T_0^{(4)}=\tfrac{1}{8}[35S_z^4-30S(S+1)S_z^2+25S_z^2-6S(S+1)+3S^2(S+1)^2],$$

and

$$T_{-4}^{(4)}=\tfrac{1}{1\,6}(70)^{\frac{1}{2}}S_-^4. \tag{11}$$

[7] B. Bleaney and K. W. H. Stevens, Repts. Progr. Phys. **16**, 108 (1953).

[8] G. Racah, Phys. Rev. **62**, 438 (1942).

The numerical values of some of the matrix elements, for $S=\frac{5}{2}$, are

$$\langle\pm\tfrac{5}{2}\mid T_0^{(4)}\mid\pm\tfrac{5}{2}\rangle=15/2,$$

$$\langle\pm\tfrac{3}{2}\mid T_0^{(4)}\mid\pm\tfrac{3}{2}\rangle=-45/2,$$

$$\langle\pm\tfrac{1}{2}\mid T_0^{(4)}\mid\pm\tfrac{1}{2}\rangle=30/2,$$

$$-\langle\tfrac{1}{2}\mid T_3^{(4)}\mid-\tfrac{5}{2}\rangle=\langle\tfrac{5}{2}\mid T_3^{(4)}\mid-\tfrac{1}{2}\rangle$$

$$=\langle-\tfrac{5}{2}\mid T_{-3}^{(4)}\mid\tfrac{1}{2}\rangle=-\langle-\tfrac{1}{2}\mid T_{-3}^{(4)}\mid\tfrac{5}{2}\rangle$$

$$=-(15/2)(14)^{\frac{1}{2}}$$

$$\langle\tfrac{3}{2}\mid T_3^{(4)}\mid-\tfrac{3}{2}\rangle=0,$$

and

$$\langle\tfrac{3}{2}\mid T_4^{(4)}\mid-\tfrac{5}{2}\rangle=(15/2)(14)^{\frac{1}{2}}. \tag{12}$$

The crystalline electric potential, given by Eq. (3), can then be written

$$V=D[S_z^2-\tfrac{1}{3}S(S+1)]-(2/45)a_0[T_0^{(4)}+b_3T_3^{(4)}-b_3^*T_{-3}^{(4)}]. \tag{13}$$

The numerical coefficient and the sign in front of a_0 were chosen in such a way that, if the crystalline potential has cubic symmetry, the ground state consists of a doublet and a quartet, the former lying lower by $3a_0$. Equation (13) indicates that at zero magnetic field the ground state consists of three doublets at

$$E=\tfrac{1}{3}D-\tfrac{1}{2}a_0\pm[(3D+\tfrac{1}{6}a_0)^2+(14/9)a_0^2\mid b_3\mid^2]^{\frac{1}{2}} \tag{14}$$

and

$$E=-\tfrac{2}{3}D+a_0.$$

In the case of solely cubic symmetry, it can be shown[9] that $b_3=(10/7)^{\frac{1}{2}}e^{i\lambda}$, in which λ is a phase factor that depends on the choice of coordinate axes. Taking $D=0$ and $b_3=(10/7)^{\frac{1}{2}}$ in Eq. (14), we obtain a quartet at a_0 and a doublet at $-2a_0$.

It is noted that the expression given by Eq. (3) can be written as a sum of an axial and a cubic field, i.e.,

$$V=V_a+V_c, \tag{15}$$

in which

$$V_a=DY_{20}-(2/45)a_0[1-\mid b_3\mid(7/10)^{\frac{1}{2}}]Y_{40}, \tag{16}$$

$$V_c=-(2/45)a_0\mid b_3\mid(7/10)^{\frac{1}{2}}\times[Y_{40}+(10/7)^{\frac{1}{2}}(e^{i\lambda}Y_{43}-e^{-i\lambda}Y_{4-3})]. \tag{17}$$

The expression V_a given by Eq. (16) is frequently referred to as the "trigonal field," despite the fact that it possesses axial symmetry. The coefficients in Eqs. (16) and (17) are related to the a and F used by Bleaney and Trenam[10]; the exact relations are $a_0=a-F$ and $\mid b_3\mid(7/10)^{\frac{1}{2}}=a/a_0=a/(a-F)$.

[9] L. M. Matarrese and C. Kikuchi, J. Phys. Chem. Solids **1**, 117 (1956).

[10] B. Bleaney and R. S. Trenam, Proc. Roy. Soc. (London) **A223**, 1 (1954).

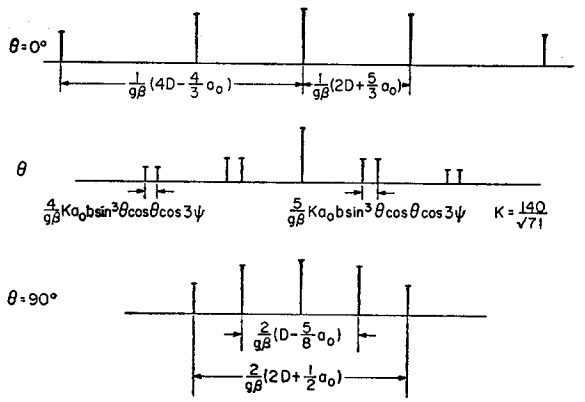

FIG. 4. Angular dependence of fine structure.

CRYSTALLINE ZEEMAN EFFECT

The expressions for the crystalline electric potential given by Eqs. (3) or (13) apply if the z axis is taken along the axis of threefold symmetry. Consequently, if the axis of quantization is taken along the magnetic field, it becomes necessary to calculate the crystalline field in terms of spherical harmonics defined in the new coordinate system. This can be done by rotating from the "crystal" into the "magnetic" coordinate system. Under this transformation each of the spherical harmonics will transform into a linear combination of spherical harmonics defined in the new coordinate system, i.e.,

$$Y_{lm}(\theta_e,\psi_e)=\sum_{m'}\gamma_{mm'}{}^{(l)}(\theta,\psi,\phi)\,Y_{lm'}(\theta_e',\psi_e'), \quad (18)$$

in which (θ,ψ,ϕ) are the Eulerian angles of the new coordinate system with respect to the old, and (θ_e',ψ_e') and (θ_e,ψ_e) are the spherical coordinates of the electron in the new and old coordinate systems, respectively. The transformation coefficients $\gamma_{mm'}{}^{(l)}$ can be expressed in terms of Jacobi polynomials.[11] However, in our present problem we shall be concerned only with the case $m'=0$, needed for the first-order perturbation calculation. The reason for this is that for Mn^{++} in calcite, when experiments are carried out at K band frequencies, the Zeeman term is large in comparison to the crystalline field terms. For $m'=0$, the Jacobi polynomials reduce to associated Legendre polynomials, so that the transformation coefficients can be written in the form:

$$\begin{aligned}
&m=0: \quad \gamma_{00}{}^{(l)}=[2/(2l+1)]^{\frac{1}{2}}\bar{P}_{l0}(\cos\theta),\\
&m<0: \quad \gamma_{m0}{}^{(l)}=[2/(2l+1)]^{\frac{1}{2}}(-1)^{m}i^{-m}e^{im\psi}\bar{P}_{lm}(\cos\theta),\\
&m>0: \quad \gamma_{m0}{}^{(l)}=[2/(2l+1)]^{\frac{1}{2}}(-1)^{m}i^{-m}e^{im\psi}\bar{P}_{l-m}(\cos\theta).
\end{aligned} \quad (19)$$

[11] E. Wigner, *Gruppentheorie und ihre Anwendung auf die Quantenmechanik der Atomspektren* (Friedrich Vieweg und Sohn, Braunschweig, 1951); now available in English translation (Academic Press, Inc., New York, 1959).

The diagonal elements of the spin Hamiltonian

$$\mathcal{H}=g\beta\mathbf{S}\cdot\mathbf{H}+A\mathbf{I}\cdot\mathbf{S}+V, \quad (20)$$

where the symbols have their usual significance, are given by

$$\begin{aligned}
&\langle Mm\,|\,\mathcal{H}\,|\,Mm\rangle=g\beta HM+AMm+D\gamma_{00}{}^{(2)}\langle M\,|\,Y_{20}'\,|\,M\rangle\\
&-(2/45)\,a_0[\gamma_{00}{}^{(4)}+b_3\gamma_{30}{}^{(4)}-b_3{}^{*}\gamma_{-30}{}^{(4)}]\langle M\,|\,Y_{40}'\,|\,M\rangle.
\end{aligned} \quad (21)$$

(Note that g and A are here regarded as isotropic; experiment [1,4] shows this to be an excellent approximation.)

The paramagnetic-resonance absorption spectrum calculated from Eq. (21) for the special values of $\theta=0°$ and $\theta=90°$ consists of six groups of five lines each, i.e., one group for each value of m, the nuclear magnetic quantum number. The decomposition of each group into five lines, called the fine structure, is illustrated in Fig. 4. The figure also shows the appearance of the group at an arbitrary θ and how the strong and weak satellites of the central component are split into doublets, whereas the central component itself remains unchanged. We now proceed to an analysis of this doublet splitting.

As pointed out earlier, the nonequivalent sites in calcite have a common axis of threefold symmetry, but are displaced from each other by a rotation about the threefold axis. If the crystalline fields at the two sites, P and Q, are given by

$$V^{(P)}=DY_{20}-(2/45)\,a_0[Y_{40}+b_3{}^{(P)}Y_{43}-b_3{}^{*(P)}Y_{4-3}], \quad (22)$$

and

$$V^{(Q)}=DY_{20}-(2/45)\,a_0[Y_{40}+b_3{}^{(Q)}Y_{43}-b_3{}^{*(Q)}Y_{4-3}], \quad (23)$$

and furthermore, if the x axis is picked so as to lie in the vertical reflection plane as shown in Fig. 3, then

$$b_3{}^{(Q)}=b_3{}^{*(P)}, \quad (24)$$

since reflection in this plane changes a P site into a Q site. Equation (24) can also be verified by an application of Eq. (4). The difference in the crystalline field at sites P and Q leads to a splitting of the fine-structure lines into doublets. The separation of the components of a doublet is

$$\begin{aligned}
&\langle M\,|\,V^{(P)}-V^{(Q)}\,|\,M\rangle-\langle M-1\,|\,V^{(P)}-V^{(Q)}\,|\,M-1\rangle\\
&=(2/45)\,a_0(b_3{}^{(P)}-b_3{}^{*(P)})\,(\gamma_{30}{}^{(4)}+\gamma_{-30}{}^{(4)})\\
&\times[\langle M\,|\,Y_{40}'\,|\,M\rangle-\langle M-1\,|\,Y_{40}'\,|\,M-1\rangle]\\
&=-(8/45)\,a_0b(105/\sqrt{7!})\,\sin^3\theta\cos\theta\cos3\psi\\
&\times[\langle M\,|\,Y_{40}'\,|\,M\rangle-\langle M-1\,|\,Y_{40}'\,|\,M-1\rangle].
\end{aligned} \quad (25)$$

For the transitions $\pm1/2\leftrightarrow\pm1/2$ (central component), the quantity in the brackets is zero, but for the transitions $\pm1/2\leftrightarrow\pm3/2$, which yield the strong satellite lines, it is $75/2$; also, $\sin^3\theta\cos\theta$ is a maximum at $\theta=60°$.

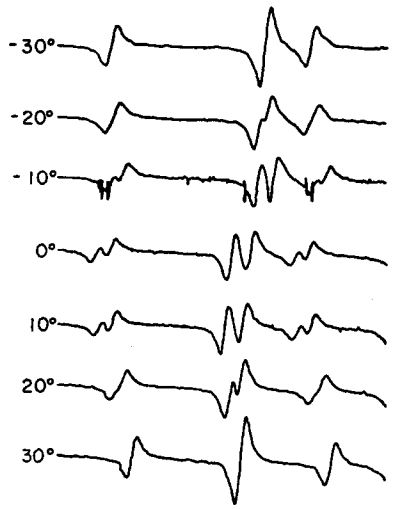

FIG. 5. Mn^{++} in calcite. Dependence of the doublet splitting on the azimuthal angle ψ. Note that the splitting is a maximum at 0°, but zero for $-30°$ and 30°.

Consequently, the expression for the numerical value of the doublet splitting at this angle becomes

$$\Delta(\pm 1/2 \leftrightarrow \pm 3/2) = (5/16)(105)^{\frac{1}{2}} \mid a_0 b \cos 3\psi \mid . \quad (26)$$

For the weak satellites $(\pm 3/2 \leftrightarrow \pm 5/2)$ the quantity in the brackets is 60/2, so that the ratio of the strong to weak doublet splittings is 5:4, in agreement with the observations by HSH. Furthermore, the angular dependence of $\sin^3\theta \cos\theta$ shows that the doublet splitting should vanish for $\theta=0$ and 90°. The dependence of the doublet splitting on the azimuthal angle ψ should be noted, being maximum and zero for $\psi=0°$ and $\psi=90°$, respectively. The case $\psi=90°$ occurs when the magnetic field lies on the vertical reflection plane.

EXPERIMENTAL PROCEDURE AND RESULTS

To check the above results, a single crystal of natural calcite containing a small concentration ($\sim$0.04%) of manganese was examined in an X band electron-spin resonance spectrometer. The spectra of Fig. 5, which shows the azimuthal dependence of the doublet splittings, were obtained by placing a calcite crystal in a rectangular TE_{012}-mode cavity in such a way as to have the c axis and the microwave magnetic field both horizontal and parallel to each other. The magnet, on a rotating mount, was swung into an appropriate position, say 70°, with respect to the crystal c axis. The crystal itself was attached to a graduated dial so that the azimuthal angle could be read accurately. Figure 5 shows that the strong and weak doublets split and coalesce with a 60° azimuthal period, as expected from the $\cos 3\psi$ dependence. Figure 6 shows an enlarged recorder trace for $\theta=70°$ and $\psi=0°$. The maximum

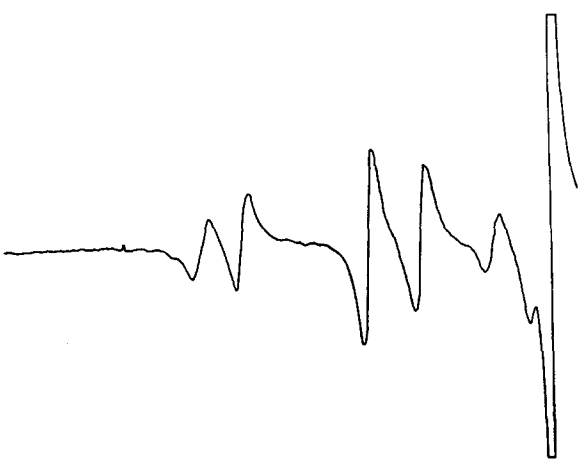

FIG. 6. Doublet splitting of the weak and strong satellites of the fine structure of Mn^{++} in calcite at $\theta=70°$, $\psi=0°$.

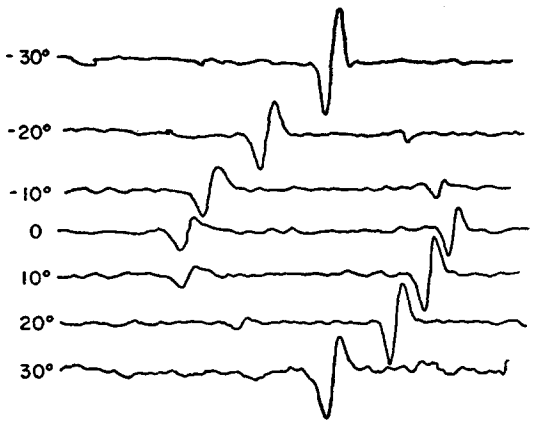

FIG. 7. Fe^{+++} in α-Al_2O_3. Dependence of the doublet splitting on the azimuthal angle ψ.

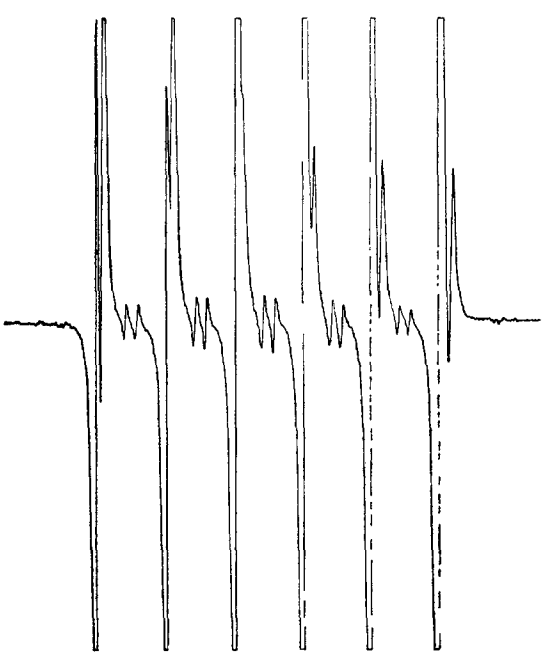

FIG. 8. Mn^{++} in calcite. The five pairs of weak lines between the hfs groups shown at high spectrometer gain.

doublet splittings are 19.3±0.5 and 15.3±0.5 gauss, respectively. This gives a ratio of 1.26±0.08; the theoretical ratio is $5/4=1.25$. These values at X band agree within experimental error with our earlier measurements at K band.[4]

In order to calculate the doublet splitting from Eq. (26) we need to know a_0 and b. The numerical value of a_0 can be obtained from the measured separations of the satellites from the central component, as indicated in Fig. 4. Using the X band data of HSH we obtain $|a_0|g\beta=7.75$ gauss, which agrees well with the value 7.85 gauss calculated from our K band experiments.[4] To evaluate b we use Eq. (6), computing the requisite quantities from the crystallographic data and assuming that the calcite structure is ionic. We find $|b|=(68.1)(7!)^{-\frac{1}{4}}$. The computed maximum splitting for the strong doublet at $\theta=60°$, $\psi=0°$, is thus 23.8 gauss. This is to be compared with the experimental value quoted above, 19.3±0.5.

Figure 7 shows the azimuthal dependence of the absorption line of Fe^{+++} in Al_2O_3. This doublet structure occurs near 5100 gauss for $\theta=60°$ at 9.35 kMc.

OTHER RESULTS

During the course of these investigations, it was discovered that the paramagnetic-resonance absorption spectrum of Mn^{++} in calcite also contains five pairs of weak lines occurring midway between the principal hfs lines (Fig. 8). These weak pairs are most clearly seen at $\theta=30°$ and $\psi=90°$ (no splitting of the fine-structure satellites). The separation between the members of a pair is about 15 gauss at K band and 24 gauss at X band. The mechanism responsible for these lines is at present somewhat uncertain. Further experimental study of these lines by one of us (L.M.M., while a visitor at Lawrence Radiation Laboratory, Livermore, California, summer, 1959) has disclosed that there are many more lines than just the five pairs already mentioned, each pair having three much weaker satellites associated with it. Moreover, there was some evidence that the positions of these satellites changed with angle. It was also noticed that these weak pairs are much more intense relative to the principal hfs lines at X band than they are at K band, and that their relaxation times were somewhat longer than those corresponding to the main-spectrum lines. The study of these lines is still in progress and will be reported at a later date.

ACKNOWLEDGMENTS

It is a pleasure to acknowledge the technical assistance of Richard Ager and James E. King.